Rotational Equilibria and Low-Order Modes of a Non-Neutral Ion Plasma

D. J. Heinzen,[a] J. J. Bollinger, F. L. Moore, Wayne M. Itano, and D. J. Wineland
Time and Frequency Division, National Institute of Standards and Technology, Boulder, Colorado 80303
(Received 4 October 1990)

We study rotational equilibria and low-order electrostatic modes of a magnetically confined, non-neutral ion plasma. The plasma rotation rate is controlled with radiation pressure from a laser beam and is continuously varied over the entire allowed range, including Brillouin flow. Excitation of an asymmetric plasma mode by a static field asymmetry is observed. The symmetric quadrupole mode is also studied; its behavior is characteristic of a strongly magnetized plasma at low density, and of an unmagnetized plasma at Brillouin flow.

PACS numbers: 52.25.Wz, 32.80.Pj, 52.35.Fp

Recently, much attention has focused on the properties of plasmas containing charges with only one sign.[1] Such non-neutral plasmas are unusually simple both theoretically and experimentally, and are unique in that steady-state thermal equilibria are possible. Nevertheless, they exhibit a wide range of collective phenomena, such as Debye shielding and collective oscillations. Typically, non-neutral plasmas are confined radially by a uniform axial magnetic field $\mathbf{B}=B\hat{\mathbf{z}}$, and axially by an electrostatic potential.[2] Such a plasma may be characterized by a self-field parameter[3] $S=2\omega_p^2/\Omega^2$, where $\omega_p=(4\pi nq^3/m)^{1/2}$ is the plasma frequency, with n, q, and m are the particle density, charge, and mass, respectively, and $\Omega=qB/mc$ is the cyclotron frequency. Of particular theoretical[1,3] and practical[4] interest is the condition $S=1$, referred to as "Brillouin flow."[3] In this state the plasma rotates rapidly about the z axis at a frequency $\Omega/2$ and is compressed to its maximum possible density of $n_B=m\Omega^2/8\pi q^2$, the "Brillouin density." Near Brillouin flow, the plasma behaves in many ways like an unmagnetized plasma.[3] Values of S near unity have been obtained in only a few experiments[5,6] where the plasma confinement times were not long enough to reach thermal equilibrium.

This paper describes the use of laser-induced torques on a magnetically confined non-neutral $^9Be^+$ plasma to access the entire range of allowed rotational thermal equilibria including Brillouin flow. Geometrical errors in the trapping fields tended to limit the range of accessible rotational equilibria. A static, azimuthally asymmetric field error was observed to excite an asymmetric collective resonance and heat the plasma. When this asymmetry was eliminated, the techniques described here were used to study a symmetric quadrupole mode of the plasma over a wide range of conditions including Brillouin flow.

The experimental apparatus (Fig. 1) has been described previously.[7] Electroformed copper cylinders produce a trap with accurate cylindrical symmetry. A potential V_T of between 10 and 300 V, applied between the end and central electrodes, confines the ions axially. The potential near the trap center is

$$V(r,z)=\frac{V_T}{d_T^2}\left(z^2-\frac{r^2}{2}\right)=\frac{m\omega_z^2}{2q}\left(z^2-\frac{r^2}{2}\right), \quad (1)$$

where $d_T=1.85$ cm and ω_z is the frequency at which a single trapped ion oscillates along the z axis. The trap is placed in a uniform magnetic field $\mathbf{B}=B\hat{\mathbf{z}}$, with $B=0.8194$ T, which confines the ions radially. The $^9Be^+$ cyclotron frequency is $\Omega/2\pi=1.40$ MHz. Background gas pressure is approximately 10^{-8} Pa. For this work, between 1000 and 5000 $^9Be^+$ ions are confined in the trap for many hours. The plasma dimensions are typically less than 0.1 cm. We remove contaminant ions with a mass-to-charge ratio greater than $^9Be^+$ by raising V_T to $\sim$550 V ($\omega_z/\Omega\sim0.67$ for $^9Be^+$). Agreement between the predicted and observed mode frequencies is obtained only when the contaminant ions are removed.

The ion plasma evolves into a near-thermal equilibrium state characterized by a uniform rotation of the plasma about the z axis at frequency ω. Under the low-temperature conditions of this experiment, the density is

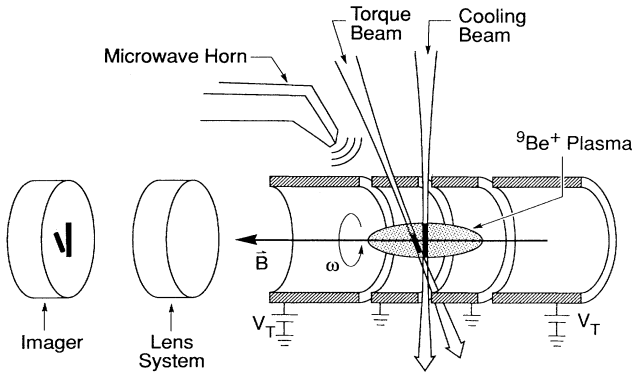

FIG. 1. Schematic drawing of the experimental apparatus. For clarity, the electrodes are shown in a cross-sectional view, and the diagonal laser beam is omitted. The size of the plasma is exaggerated.

uniform over length scales large compared to the interparticle spacing and the plasma frequency is given by $\omega_p^2 = 2\omega(\Omega - \omega)$.[8] The density falls to zero at the boundary of the plasma in a distance on the order of the Debye length,[9] which in our experiment is much less than the plasma dimensions. With the confining potential of Eq. (1), the plasma boundary is spheroidal with an aspect ratio $\alpha \equiv z_0/r_0$ determined by ω from the expression $\omega_z^2 = \omega_p^2 Q_l^0(\alpha/(\alpha^2-1)^{1/2})/(\alpha^2-1)$.[8] Here $2z_0$ and $2r_0$ are the maximum axial and radial extent of the plasma and Q_l^m is the associated Legendre function of the second kind. We neglect the effect of image charges because the plasma dimensions are much smaller than the trap dimensions.

The plasma density and temperature are controlled with radiation pressure from two cw laser beams nearly resonant with the $2s\,^2S_{1/2}(m_I = +\frac{3}{2}, m_J = +\frac{1}{2}) \rightarrow 2p\,^2P_{3/2}(+\frac{3}{2}, +\frac{3}{2})$ transition of $^9Be^+$ at frequency ω_0 ($\lambda \approx 313$ nm), where m_I and m_J are the nuclear- and electron-spin projections along $\hat{\mathbf{z}}$. One of these, the "cooling beam," is tuned 10–50 MHz below ω_0, has a power of 50–500 μW, and is directed through the plasma center in a direction perpendicular to the z axis. The second beam, the "torque beam," is directed perpendicularly to the z axis through the side of the plasma that recedes from the laser beam (Fig. 1). Its frequency ω_T is between 0 and 1500 MHz above ω_0 and its power is 1–3 μW. For some of the measurements, a third laser beam is directed diagonally through the plasma with a component along $\hat{\mathbf{z}}$, to provide additional laser cooling.[7] Each beam diameter is 25–50 μm, an order of magnitude less than the typical plasma diameter. The torque beam supplies energy to the plasma and provides a torque which changes the plasma angular momentum and increases ω. Equilibrium is maintained because the energy input by the torque beam is removed by the cooling beam,[10] and because the laser-beam torques and torques from static field asymmetries sum to zero.[11–13] Temperatures typically below 250 mK are obtained.

Light scattered from the ions is imaged by a lens system onto a photon-counting imaging tube.[7] A real-time display of the image is used to monitor the plasma kinetic energy; a hot plasma has a more diffuse boundary and less ion fluorescence. With this simple diagnostic we did not, in general, distinguish between an increase in the random thermal energy of the ions and the excitation of coherent modal motion of the ions. In order to measure the rotation frequency of the plasma, we drive the $(+\frac{3}{2}, +\frac{1}{2}) \rightarrow (+\frac{3}{2}, -\frac{1}{2})$ electron spin-flip transition of the $^9Be^+$ ground state at $\omega_s/2\pi \simeq 22$ GHz. The transition is observed as a decrease in the ion fluorescence.[14] Absorption at both the "carrier" frequency ω_s and the motional "sideband" frequencies $\omega_s \pm \omega$ are observed. These sidebands occur because the ions see the microwave field as being phase and amplitude modulated at frequency ω, due to the coherent rotational motion of the ions.[15] The rotation frequency $\omega/2\pi$ is determined to an accuracy of approximately 5 kHz.

With the two-laser-beam technique, we are able to establish a stable rotation frequency at any value in the allowed range from ω_m to $\Omega - \omega_m$, where $\omega_m = \Omega/2 - (\Omega^2/4 - \omega_z^2/2)^{1/2}$ is the single-ion magnetron frequency.[8] Initially, with ω small, the torque laser frequency ω_T is tuned near ω_0, and the torque beam induces very little fluorescence due to the rotation-induced Doppler shift. Then, as ω_T is slowly increased, the ion fluorescence and torque increase, and the plasma compresses and rotates faster. For $\omega < \Omega/2$, the plasma radius decreases and the aspect ratio α increases with increasing ω. A typical curve of rotation frequency versus torque laser tuning is shown in Fig. 2. At high rotation frequencies hysteresis occurs. On the lower branch (increasing ω_T), the plasma becomes much hotter and rotates at a nearly constant frequency, until an abrupt transition to a cold state of faster rotation occurs. With further increases in ω_T, the rotation frequency can be smoothly varied through Brillouin flow ($\omega = \Omega/2$) to frequencies slightly less than $\Omega - \omega_m$. For $\omega > \Omega/2$, the plasma radius increases and the aspect ratio decreases with increasing ω. On the upper branch of the hysteresis (decreasing ω_T), the rotation frequency decreases smoothly, and the plasma remains cold until some heating is again observed, at a rotation frequency slightly higher than that at which heating first occurred on the lower branch. The size of the hysteresis depended sensitively on the angle θ_0 between the trap symmetry axis and the magnetic field. For $\theta_0 > 0.1°$, the plasma rotation frequency could not be increased beyond the point at which heating first occurred. We could make $\theta_0 < 0.01°$ by searching for an alignment which gave no apparent heating or hysteresis.

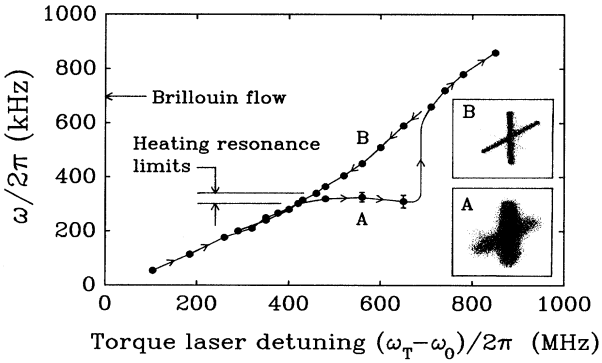

FIG. 2. Plasma rotation frequency as a function of torque laser frequency. Arrows indicate the direction of the frequency sweep. Insets *A* and *B* illustrate the appearance of hot and cold plasmas, respectively. Image *A* was recorded on the lower branch of the hysteresis, and image *B* on the upper. Bright fluorescence from the cooling and diagonal beams, and weak fluorescence from the torque beam, is visible.

The rotation frequency ω at which heating occurs for $\theta_0 \simeq 0.02°$ is shown in Fig. 3 as a function of ω_z. The lower bounds indicate where heating first occurs with increasing rotation frequency and the upper bounds indicate where heating first occurs with decreasing rotation frequency. We have identified this heating resonance as an excitation of a collective $(l,m)=(2,1)$ plasma mode by the static field asymmetry associated with the trap-magnetic-field misalignment. [The indices l and m refer to a description of the modes in spheroidal coordinates, with m describing the azimuthal (ϕ) variation, and l the variation along a spheroidal surface in the direction perpendicular to $\hat{\phi}$.] This mode is similar to an $m=1$ diocotron mode in a cylindrical plasma column with a wavelength equal to the plasma length.[16] In this mode the plasma density remains constant and the shape spheroidal, but the plasma symmetry axis is tilted with respect to the z axis and precesses backwards relative to the plasma rotation at frequency ω. That is, the mode frequency $\omega_{21}^{(\mathrm{rot})}$ in the rotating frame is negative. Therefore when $\omega_{21}^{(\mathrm{rot})}=-\omega$, the mode has frequency $\omega_{21}=0$ in the laboratory frame and may be excited by static field asymmetries.[11-13] We show as a solid line in Fig. 3 the calculated rotation frequency ω at which $\omega_{21}=0$. Excellent agreement between the predicted and observed rotation frequencies is obtained. We calculate[17] ω_{21} by considering small axial and radial displacements of the ions from their equilibrium positions consistent with a tilt of the plasma symmetry axis. A self-consistent calculation of the axial and radial restoring forces to first order gives two linear differential equations describing the motion of the axial and radial displacements. The requirement that the eigenfrequencies for these two equations be equal gives a cubic equation for ω_{21}.

A static field error cannot transfer energy to the plasma. However, it can convert potential energy to thermal energy by producing a radial expansion of the plasma. In our work, the laser beams are sources of strong torques and energy input as well as cooling. We have not attempted to model all of the energy input and torques and obtain a quantitative description of the radial transport and heating produced by the static (2,1) mode.

We have also measured the (2,0) axially symmetric quadrupole mode frequency of the plasma. This mode is similar to an $m=0$ plasma mode in a cylindrical plasma column with a wavelength equal to the plasma length. In this mode the plasma density remains uniform and the shape spheroidal, but the plasma aspect ratio α oscillates in time. The mode is excited with an oscillating potential applied between the trap's end and center electrodes and resonance is observed by a change in the ion fluorescence. Results are shown in Fig. 4 for two different trap potentials. The solid line shows the mode frequency ω_{20} calculated in a manner similar to the (2,1) mode and given by[17]

$$2\omega_{20}^2=\Omega_u^2+\omega_Q^2-\{(\Omega_u^2-\omega_Q^2)^2-4\Omega_v^2(\omega_z^2-\omega_Q^2/3)\}^{1/2}. \quad (2)$$

Here $\Omega_v=\Omega-2\omega$ is the vortex frequency, $\Omega_u=(\Omega_v^2+\omega_p^2)^{1/2}$ is the upper hybrid frequency, and $\omega_Q^2=\omega_p^2\times 3\alpha Q_2^0(\alpha/(\alpha^2-1)^{1/2})/(\alpha^2-1)^{3/2}$. The frequency ω_Q is the (2,0) mode frequency in the absence of a magnetic field (i.e., a plasma confined by a uniform background of opposite charge). Again, good agreement between the predicted and observed mode frequencies is obtained with no adjustable parameters. Independently, a more general calculation of spheroidal plasma mode frequencies has been recently carried out by Dubin.[18]

Figure 4 shows two additional calculations. In the

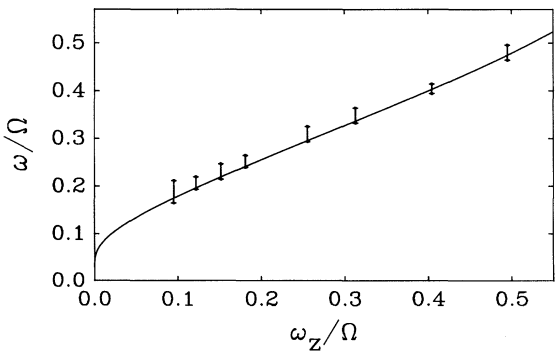

FIG. 3. Rotation frequency ω at which heating was observed as a function of the single-particle axial frequency ω_z. Both frequencies are expressed in units of the cyclotron frequency Ω. The error bars on the measurements are explained in the text. The solid line indicates the calculated rotation frequency ω at which $\omega_{21}=0$. This is a universal curve involving no adjustable parameters.

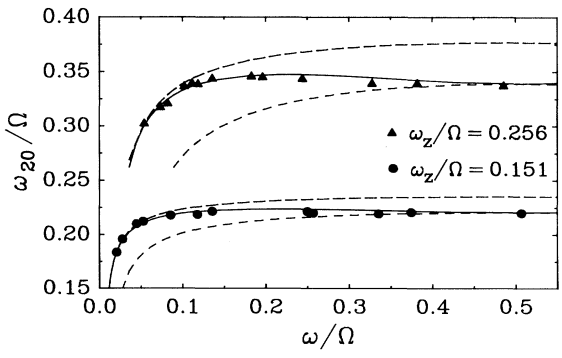

FIG. 4. Plasma quadrupole frequency ω_{20} as a function of rotation frequency ω for $\omega_z/\Omega=0.151$ ($V_T=28$ V) and $\omega_z/\Omega=0.256$ ($V_T=80$ V). All frequencies are expressed in units of the cyclotron frequency Ω. The circles and triangles give the experimental data. The solid lines give the cold-fluid model predictions for ω_{20}. The dashed and dotted lines give the high- and low-magnetic-field calculations for ω_{20}, respectively.

first, shown as dashed lines, the magnetic field is assumed to be effectively infinite; that is, the ions are not allowed to move radially, and the mode frequency is calculated assuming a simple axial stretch of the charged spheroid. In the second, shown as dotted lines, the magnetic field is assumed to be effectively zero; that is, the curve shows ω_Q. The quadrupole mode frequency varies smoothly from the high-magnetic-field calculation at low rotation frequencies to the zero-magnetic-field calculation at the Brillouin limit.

We also studied plasmas containing about 40000 $^9Be^+$ ions at a magnetic field $B=6$ T ($n_B=1.1\times10^{10}$ cm^{-3}) and trap voltage $V_T=500$–1500 V. At this field, we were also able to obtain rotation frequencies throughout the allowed range. The (2,1) heating resonance was much stronger and more sensitive to the magnetic-field alignment. In addition, weaker heating resonances, which were also sensitive to the magnetic-field alignment, were observed at lower rotation frequencies than the (2,1) heating resonance. We were unable to remove contaminant ions from the plasma at this high magnetic field.

In conclusion, we have shown that the entire range of allowed rotational equilibria can be realized in a non-neutral ion plasma using laser-induced torques and by careful control of trap asymmetries. This should permit detailed investigations of non-neutral plasmas near Brillouin flow. Here we studied the excitation of an asymmetric tilt mode of the plasma by a static field asymmetry. This mode heated the plasma and tended to limit the plasma density. Observation of this mode allows the magnetic- and electric-field axes to be carefully aligned. We also studied a symmetric quadrupole mode and showed that the plasma exhibits unmagnetized behavior near Brillouin flow. Measurement of this mode frequency, perhaps through induced image currents in the trap electrodes,[19] could provide useful information on plasma rotation frequency, shape, and density when the plasma cannot be directly imaged.

We gratefully acknowledge the support of the Office of Naval Research. We also thank Dan Dubin and Fred Driscoll for stimulating conversations, and Sarah Gilbert and Jim Bergquist for their comments on the manuscript.

---

[a]Current address: Department of Physics, University of Texas, Austin, TX 78712.

[1]*Non-Neutral Plasma Physics,* Proceedings of the Symposium of Non-Neutral Plasma Physics, Washington, D.C., 1988, edited by C. W. Roberson and C. F. Driscoll, AIP Conf. Proc. No. 175 (AIP, New York, 1988).

[2]J. H. Malmberg and J. S. deGrassie, Phys. Rev. Lett. **35**, 577 (1975).

[3]R. C. Davidson, *Physics of Nonneutral Plasmas* (Addison-Wesley, Reading, MA, 1990); R. C. Davidson, in *Non-Neutral Plasma Physics* (Ref. 1).

[4]Wayne Vernon, in *Proceedings of the Workshop in Intense Positron Beams, Idaho Falls, Idaho, 1987,* edited by E. H. Ottewitte and W. Kells (World Scientific, Singapore, 1988), p. 135.

[5]A. J. Theiss, R. A. Mahaffey, and A. W. Trivelpiece, Phys. Rev. Lett. **35**, 1436 (1975).

[6]Guy Dimonte, Phys. Rev. Lett. **46**, 26 (1981).

[7]S. L. Gilbert, J. J. Bollinger, and D. J. Wineland, Phys. Rev. Lett. **60**, 2022 (1988).

[8]L. R. Brewer, J. D. Prestage, J. J. Bollinger, W. M. Itano, D. J. Larson, and D. J. Wineland, Phys. Rev. A **38**, 859 (1988).

[9]C. F. Driscoll, J. H. Malmberg, and K. S. Fine, Phys. Rev. Lett. **60**, 1290 (1988).

[10]W. M. Itano, L. R. Brewer, D. J. Larson, and D. J. Wineland, Phys. Rev. A **38**, 5698 (1988).

[11]Rhon Keinigs, Phys. Fluids **24**, 860 (1981); **27**, 1427 (1984).

[12]C. F. Driscoll and J. H. Malmberg, Phys. Rev. Lett. **50**, 167 (1983).

[13]D. L. Eggleston, T. M. O'Neil, and J. H. Malmberg, Phys. Rev. Lett. **53**, 982 (1984).

[14]D. J. Wineland, J. C. Bergquist, W. M. Itano, and R. E. Drullinger, Opt. Lett. **5**, 245 (1980).

[15]H. S. Lakkaraju and H. A. Schuessler, J. Appl. Phys. **53**, 3967 (1982).

[16]S. A. Prasad and T. M. O'Neil, Phys. Fluids **26**, 665 (1983).

[17]J. J. Bollinger *et al.* (to be published).

[18]D. Dubin, preceding Letter, Phys. Rev. Lett. **66**, 2076 (1991).

[19]D. J. Wineland and H. Dehmelt, Int. J. Mass Spectrom. Ion Phys. **16**, 338 (1975); **19**, 251 (1976).